Test	k_1 (PT)	k_2 (PT)	k_1 (SE)	k_2 (SE)
(1 pig)	(m/s) $\times 10^7$	(m/s) $\times 10^5$	(m/s) $\times 10^7$	(m/s) $\times 10^5$
—	9.5 (0.3)	5.4 (0.4)	8.7 (0.3)	20.0 (0.4)
CP89	10.0 (0.3)	18.0 (0.4)	12.0 (0.3)	13.0 (0.4)
CP90	6.6 (0.3)	5.9 (0.4)	13.0 (0.3)	1.0 (0.4)
CP92	10.0 (0.3)	16.0 (0.4)	12.0 (0.3)	7.5 (0.4)
CP98	6.6 (0.3)	7.2 (0.4)	7.1 (0.3)	9.8 (0.4)

Table 2. MBL model parameters. The top row shows the values for k_1 and k_2 obtained considering all the available data for which the model can produce a prediction (no stenosis). The remaining rows show the values obtained for the cross-validation analysis. PT—pig tendon; SE—subendothelium.

Test	β_C	β_t	β_γ	$\beta(T)$
—	2.2(0.3)	1.4(0.1)	0.38(0.07)	−6.4(0.8) (PT) −6.7(0.8) (SE) −5.3(0.8) (TM)
CP89	2.2(0.3)	1.3(0.1)	0.42(0.08)	−6.4(0.8) (PT) −6.3(0.8) (SE) −5.8(0.8) (TM)
CP90	2.1(0.3)	1.3(0.1)	0.30(0.09)	−5.7(0.9) (PT) −5.8(0.9) (SE) −5.2(0.9) (TM)
CP92	2.6(0.5)	1.7(0.1)	0.40(0.08)	−8.0(1.0) (PT) −8.0(1.0) (SE) −7.0(1.0) (TM)
CP98	2.0(0.4)	1.3(0.1)	0.40(0.09)	−6.0(1.0) (PT) −6.0(1.0) (SE) −5.0(1.0) (TM)

Table 3. PM parameters. The top row shows the values [value (error)] for β_C (platelet concentration), β_t (perfusion time), β_γ (shear rate) and $\beta(T)$ (tissue) obtained considering all the available data. The remaining rows show the values obtained for the cross-validation analysis considering data for the specified pig as the test set and data for the remaining pigs as the training set. PT—pig tendon; SE—subendothelium, TM—tunica media.

Our analysis shows that the three approaches we propose produce reasonable predictions of the amount of deposited platelets (Fig. 4). Note that we can build further confidence in the MBL and PM because model parameters show little variation (that is, are always in the same orders of magnitude) across the set of cross-validations. We note that in the PM all parameters in Eq (1) are significantly different from zero. In addition, in the case of pig tendon and subendothelium, the tissue parameters ($\beta(T)$ in Eq (1)) are very similar, confirming that there is little difference in platelet deposition on these two substrates as expected.

In order to quantify the predictive power of each one of the approaches, we compute the relative error for each one of the cross-validations performed with the three approaches (Fig. 5 and Supporting Figure S1-5). We note that the median error is typically low, and that the PM is the model that performs best. On average the PM shows relative errors typically about 14.2%, while MBL and RF approaches have median errors of 21% and 20.7%, respectively. This is also the case if we only consider data points for which MBL can produce predictions (that is, experiments with no stenosis), for which the PM has an average median error of 12.9%, while MBL and RF approaches on average have median errors of 22% and 17.2%, respectively.

We also note that in one of the cases (when predicting platelet deposition for pig CP92) we find that the RF and PM approaches have a much lower predictive power. An inspection of the data reveals that this dataset has a narrow range of platelet deposition values—CP92 platelet deposition: (platelets/cm$^2 \times 10^{-6}$) [2.4, 135.3]—, while the rest of data has a wider range—[0.62, 2013.74] (platelets/cm$^2 \times 10^{-6}$)—and that values are lower for CP92 ([182.0, 287.07] (platelets/μl $\times 10^{-3}$) than for the other three pigs (platelet

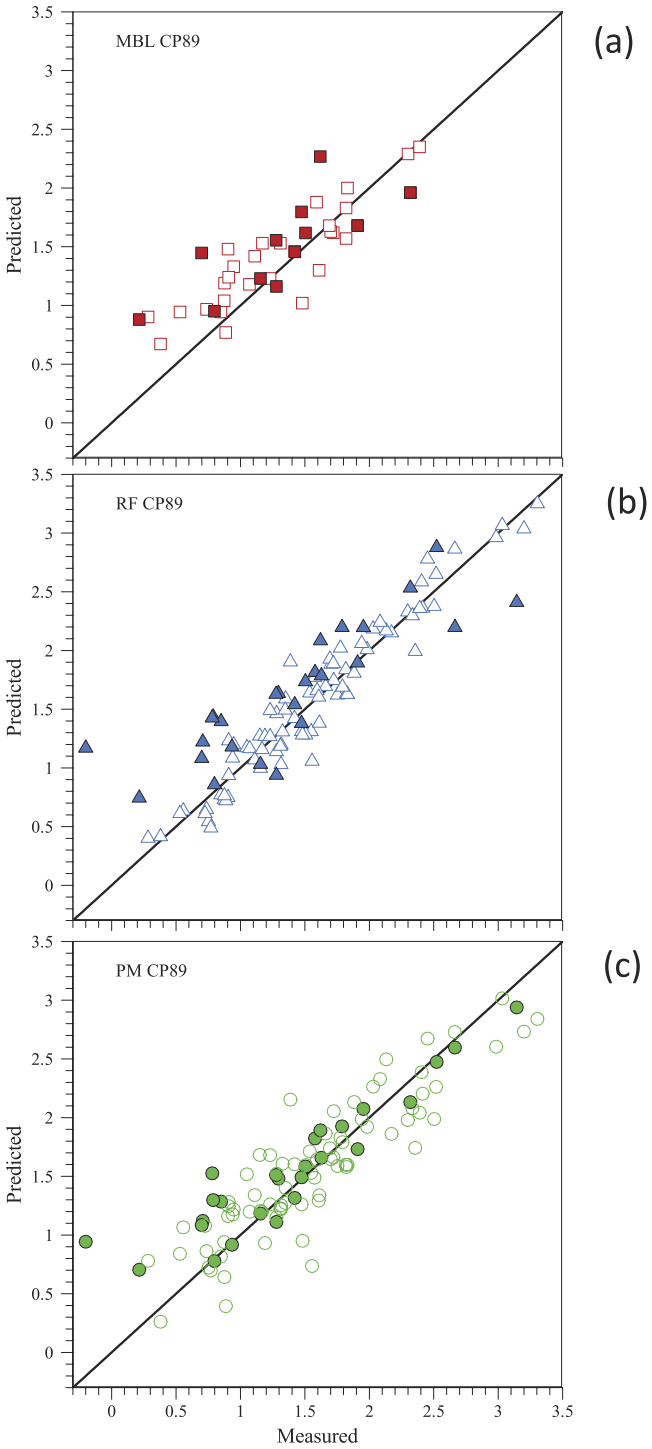

Figure 3. Cross-validation plot for pig CP89 showing platelet deposition predicted by (**a**) the mass-boundary layer model (MBL, red squares), (**b**) Random forest (RF, blue triangles) and (**c**) the phenomenological model (PM, green circles). We show model predictions as $\log_{10}$(number of platelets/$\text{cm}^2 \times 10^{-6}$) versus the corresponding experimental values for which MBL can produce a prediction (no stenosis). Open symbols correspond to the training set and filled symbols correspond to the test set. Parameters for PM: $\beta(T) = -6.3$ (PT), -6.3 (SE), -5.8 (TM), $\beta_C = 2.2$, $\beta_t = 1.33$, $\beta_\gamma = 0.402$.

concentration [289.07, 498.89] (platelets/μl $\times 10^{-3}$). Therefore, the loss of predictive power is probably due to the fact that the training data set has 'less' information in the region where CP92 points lie since the training set covers a broader range. This issue highlights the importance of the training set in order to obtain accurate predictions.

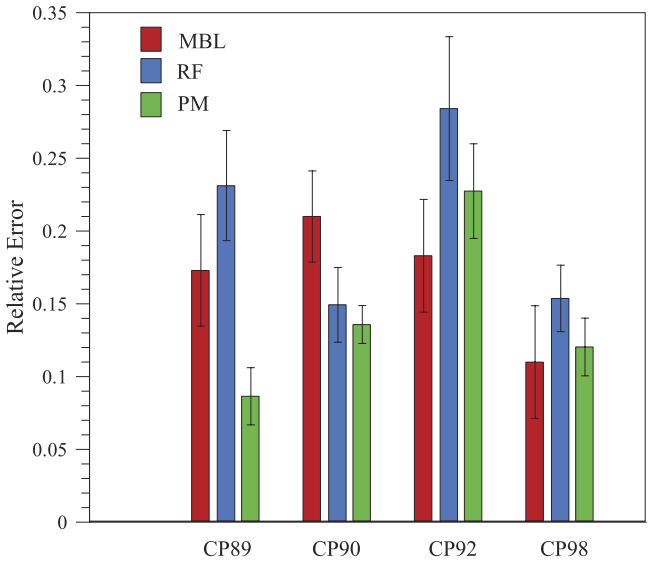

Figure 4. Median relative error in the test sets. For each one of the cross-validation analysis we show the median relative error: difference between the predicted and the measured value, relative to the measured value. Error bars correspond to median absolute deviation divided by the square root of observations. For each one of the approaches: MBL—Mass Boundary Layer Model, RF—Random Forest and PM—phenomenological model.

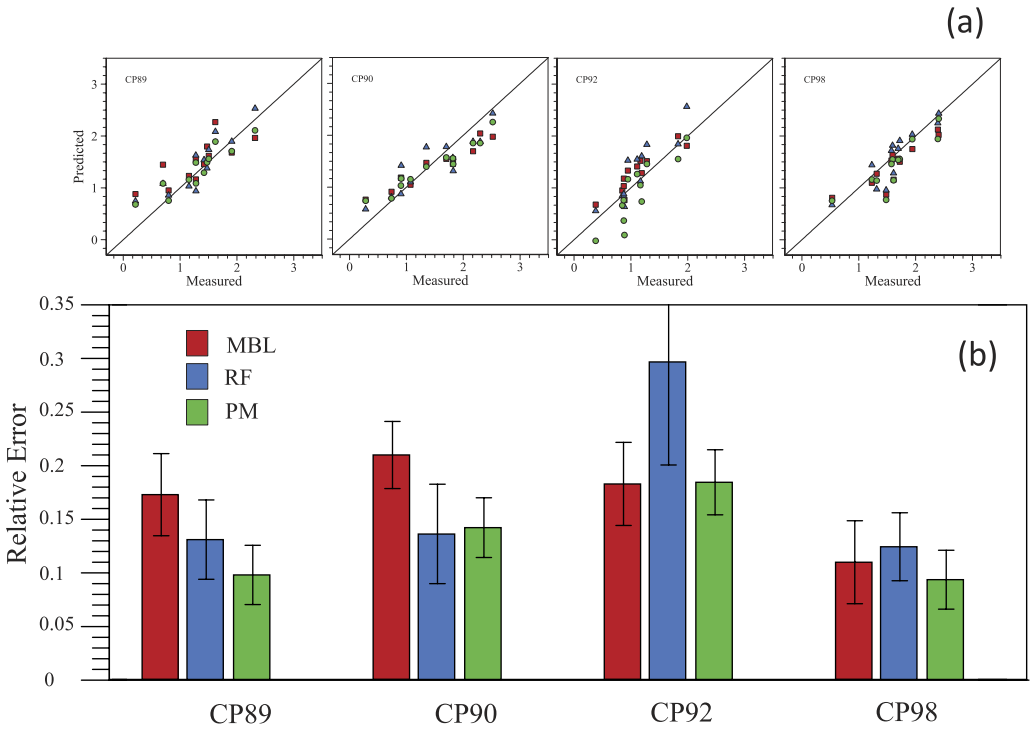

Figure 5. (**a**) Prediction and true value of platelet deposition of test sets. We use the same data points in each test set to directly compare the three modelling methods. (**b**) Median error of previous cross-validation, relative error: difference between the predicted and the measured value, relative to the measured value. Error bars correspond to median absolute deviation (MAD) divided by the square root of observations. MBL: Mass Boundary Layer (squares) Model, RF = Random Forest (Triangles), PM = Phenomenological Model (circles).

Discussion

Our study showcases the validity of computational approaches to predict platelet deposition in vascular tissues in a number of different conditions. First, we empirically assessed platelet deposition exposing animal blood to a thrombus triggering substrate during different time periods and at different shear rates. Then, we tested the predictive power of three complementary approaches: i) a principle based approach using a mass-transfer model; ii) a machine learning approach that has no information about the physico-chemistry behind the biological process (Random Forest); iii) a phenomenological model constructed from empirical evidence.

Our study shows that the three approaches have a consistent predictive power, the phenomenological model having an overall better performance. Furthermore, our analysis highlights the main advantages and disadvantages of the different approaches (see Fig. 1).

Our analysis also shows that RF and PM approaches would significantly benefit from the availability of platelet deposition data for a larger variety of empirical conditions (for instance, different shear rates and perfusion times). However, this is not necessarily the case for the MBL model. The assumptions made in such model impose certain limitations on the range of applicability of the model. In particular, our MBL approach is not applicable to cases with stenosis or for long times of perfusion when platelet detachment may occur (see for example Supporting Figure S1-4c, where a decrease of deposited platelets is observed for perfusion times between 10 and 30 minutes). The extension of the range of applicability of the MBL model to these cases would require to take into account and parametrize a) the variation of the wall shear rate along the substrate with stenosis and b) the mechanisms responsible for the platelet detachment, thus entailing an increase in the number of fitting parameters.

The availability of a larger variety of empirical conditions would help improve the prediction power of the PM in two aspects. One the one hand, it would yield a more robust set of model parameter values that would give good predictions for a larger range of empirical conditions. On the other hand, new experimental data could help uncover new empirical facts that could be used to refine our model.

Finally, our study shows that the parameter based approaches we propose are biologically sound. Remarkably, our mass-transfer model is a novel model that built upon common approaches in literature that explicitly differentiates between the formation of the first monolayer and that of the subsequent layers. The fact that the kinetic constants associated to each of these mechanisms are different by an order of magnitude indicates that this is an important aspect of the platelet deposition process. In the PM, the fact that all the model parameters are different from zero all the variables we selected have a distinct impact in the platelet deposition process. Additionally, for both approaches we obtain parameter values that are consistent with our expectation of the differences of deposition on different substrates. In particular, in the PM approach tissue dependency is well captured by a single parameter that is similar for pig tendon and subendothelial tissues and different for the tunica media. In contrast, the parameters associated to shear rate, platelet concentration in blood, and perfusion time remain the same throughout the analysis. In fact, according to Table 3 the largest contribution is that of platelet concentration in blood and perfusion time, which is also consistent with the assumptions in the MBL model.

All in all, our study opens the door toward further studies that aim to integrate macroscopic description of the models we propose by coupling it to more refined models of the microscopic processes behind platelet deposition.

Methods

Data description and prediction experiments. *Experimental animal model.* Experiments were performed in Large White x Landrace commercial pigs ($n = 4$, $m \approx 36$ kg), individually caged in a light-, temperature-, and humidity-regulated environment with controlled feeding and free access to water. The investigation conforms to the Guide for the Care and Use of Laboratory Animals published by the US National Institute of Health (NIH Publication No. 85-23, revised 1996).

Radioactive labeling of platelets. We performed radioactive labeling of platelets to monitor their deposition (monolayer and multilayer). To that purpose, after overnight fasting, 43 ml of pig blood was drawn in 7 ml of anticoagulant citrate dextrose solution by femoral venipuncture. Platelets were isolated and labeled with ^{111}In (Amersham Biosciences, UK) as described in[25] suspended in a final volume of 4 ml of autologous plasma, and reinjected into the pig (ear vein) within 2 h. Labeling efficiency was around 90% and the injected activity was around 250 microCi. Post-mortem ^{111}In biodistribution indicated a correct platelet distribution with maximal accumulation in blood.

Extracorporeal perfusion system in the Badimon chamber. The study protocol was approved by the institutional ethics committee (CSIC-ICCC) and all animal procedures were performed conform the guidelines from Directive 2010/63/EU of the European Parliament on the protection of animals used for scientific purposes or the NIH guidelines. In addition, we have followed the ARRIVE guidelines[38]. We assessed platelet behavior by exposing the animal blood to a thrombus triggering substrate during different time periods and at different shear rates in the previously validated and standardized Badimon perfusion chamber[21]. To that end, after overnight fasting, animals were tranquilized (8 mg kg^{-1} Stressnil, Esteve), anesthetized (10 mg kg^{-1}, B. Braum, Spain), and a carotid artery-jugular vein shunt was established to place the Badimon perfusion chamber as previously described[25]. All of the animals received

low-dose anticoagulation with heparin (50 IU kg^{-1}) as a continuous infusion to avoid clotting inside the tubing system. This heparin regime does not affect platelet deposition[21].

Blood was perfused through the chamber for different time periods (3, 5, 10, 20 and 30 minutes) at shear rates of 212 s^{-1}, 1690 s^{-1} and at an experimental stenosis of 80%, that corresponds to a shear value of 1390 s^{-1}, in order to mimic the rheological conditions within blood vessels (see the following section for details on the calculation of these values). The thrombogenic substrates (platelet-triggering surfaces) included homologous porcine vessel walls with 2 types of damage [mild (denuded vessel wall or sub-endothelium SE) and severe (disrupted vessel wall or tunica media TM)] and pig tendon (PT). Several perfusions with varying time of perfusion, hemodynamic conditions and triggering substrate were performed in each animal. After the perfusion, vessels were fixed in 4% paraformaldehyde to count labelled platelets using a gamma counter (Wizard, Wallac, USA). Values were normalized by blood ^{111}In activity (counts), platelet counts in blood, and area exposed surface[25]. At the end of the experiment, animal's heart was arrested with a 10 ml potassium chloride 2M intravenous injection.

Hematological and hemodynamic parameters. We determined hematocrit and platelet count throughout the experimental period with as System 9000 Serono cell analyzer.

Overview of the data. Table 1 provides an overview of the type and range of data collected from the experiments.

For the perfusions performed with 80% of stenosis, we computed the shear rate solving numerically the Navier-Stokes equations in the three dimensional domain that emulate the perfusion chamber with and without the stenosis (see S3 for details).

An analysis of the empirically measured platelet deposition counts reveals that the distribution of the logarithm of the number of deposited platelets has no gaps and is smoother than the distribution of the number of deposited platelets (see Figure. S1-1). For this reason, we focus on predicting the $\log_{10}$ of the number of deposited platelets.

Computational approaches to platelet deposition. *Mass-transfer boundary-layer model (MBL).* Convection-diffusion-reaction models assume that the platelet deposition rate is proportional to a reaction kinetics constant and to the platelet concentration at the wall[8,10,27–31,39–43]. In here, we consider a generalization of a simple model of platelet deposition that includes implicitly the effect of the convective force using boundary-layer theory and differentiates between the first monolayer of platelet deposition [platelet in contact with the substrate (e.g. endothelial layer)] and the following multi-layer platelet aggregates (platelet-platelet interaction and thrombus growth).

Specifically, in our model we assume two different kinetic reaction constants: k_1 for the formation of the first monolayer and k_2 for the formation of subsequent layers. Therefore, we consider that as the first layer is being covered, with a maximum number of platelets $P_\infty = \frac{4A}{\pi d_p^2}$ where $A = \delta W$ is the area of the substrate and $d_p = 2\times10^{-6}$ m is the diameter of an adhered platelet[10], the second layer starts to form. We model the two adhesion processes with first order kinetics.

In our model, for each one of the layers i we consider, the platelet deposition rate N_i'' given certain wall flux of platelets depends on the available deposition area WL_i,

$$\frac{dP_i}{dt} = N_i'' W L_i \quad i = 1, 2 \tag{2}$$

with $L_1 = \delta\left(1 - \frac{P_1}{P_\infty}\right)$ and $L_2 = \delta\frac{P_1}{P_\infty}$

We assume that the diffusion, advection and reaction processes occur within a two-dimensional mass transfer boundary layer much thinner than the diameter of the perfusion chamber; and that there is a defect of concentration of platelets in comparison with the bulk concentration in the blood (see Supporting Material S2 for a full derivation and for a discussion about the physical interpretation of the equations), the platelet flux on a substrate of length L can be written as[26] (see Supporting Material S2),

$$N_i'' = \frac{C_0}{\frac{1}{k_i} + 1.238\left(\frac{L_i}{\gamma D^2}\right)^{1/3}} \quad i = 1, 2 \tag{3}$$

where C_0 is the bulk concentration of platelets in the blood flow, γ is the shear rate, which is assumed to be constant within the mass transfer boundary layer thickness and D is the diffusion coefficient that depends on the hematocrit concentration[44] (see Supporting Material S2).

To numerically determine the kinetic constants using the MBL model, we assume that k_1 depends only on the type of substrate used in the experiments. For each set of experiments with a given substrate, we then compute the time evolution of P_1 and P_2 (see Eqs. S2-10 and S2-11). We then perform the calculations for several values of k_1 and k_2 in the ranges $10^{-3} \le k_1 \le 10^{-8}$ m/s and $10^{-3} \le k_2 \le 10^{-8}$ m/s. For each pair of values (k_1, k_2), we then compute the absolute difference between the predicted value of the total number of platelets deposited and the corresponding experimental value at a given time. For each

different substrate, we select the pair of values (k_1, k_2) that minimizes the absolute difference between the measured and predicted values.

Random Forest (RF). We use Random Forest to predict the $\log_{10}$ of the platelet deposition count using four quantitative features and two qualitative features (see Table 1). In our analysis, we used the Random Forest Package version 4.6–7[45] within R version 3.0.2[46]. We set the algorithm to the following parameters (mtry $=\sqrt{6}$, ntree $=1000$). In order to control for the slight variation of each forest due to the bagging process, we performed 100 times each RF. For the estimation of the feature importance, we leaved one feature out of the Random Forest and computed the error rate. Additionally, we applied a linear correction to initial RF predictions to improve the error rate (see Supporting Figure S1-2).

Phenomenological model for platelet deposition (PM). We estimate the parameters by performing a least-squares fit of the data using the R software[46].

References

1. Nichols, M. *et al.* European cardiovascular disease statistics 2012. http://www.escardio.org/about/documents/eucardiovascular-disease-statistics-2012.pdf (2012). European Heart Network, Brussels;European Society of Cardiology, Sophia Antipolis. Date accesed: 12/10/2014.
2. Vandrangi, P., Sosa, M., Shyy, J. & Rodgers, V. Flow-dependent mass transfer may trigger endothelial signaling cascades. *PLoS ONE* **7,** e35260 (2012).
3. Jordan, D., Homer-Vanniasinkam, S., Graham, A. & Walke, R. P. The effects of margination and red cell augmented platelet diffusivity on platelet adhesion in complex flow. *Biorheology* **41,** 641–53 (2004).
4. Skorczewski, T., Erickson, L. & Fogelson, A. Platelet motion near a vessel wall or thrombus surface in two-dimensional whole blood simulations. *Biophys J* **104,** 1764–72 (2013).
5. Badimon, L., Padro, T. & Vilahur, G. Extracorporeal assays of thrombosis. *Methods Mol Biol.* **788,** 43–57 (2012).
6. Badimon, L. & Vilahur, G. Thrombosis formation on atherosclerotic lesions and plaque rupture. *J Intern Med.* **276,** 618–32 (2014).
7. Cito, S., Mazzeo, M. & Badimon, L. A review of macroscopic thrombus modeling methods. *Thromb Res* **131,** 116–24 (2013).
8. Affeld, K., Goubergrits, L., Watanabe, N. & Kertzscher, U. Numerical and experimental evaluation of platelet deposition to collagen coated surface at low shear rates. *J Biomech* **46,** 430–36 (2013).
9. Kulkarni, S. *et al.* A revised model of platelet aggregation. *J Clin Invest* **105,** 783–91 (2000).
10. Tokarev, A., Butylin, A. & Ataullakhanov, F. Platelet adhesion from shear blood flow is controlled by near-wall rebounding collisions with erythrocytes. *Biophys J* **100,** 799–808 (2011).
11. Weller, F. Platelet deposition in non-parallel flow: influence of shear stress and changes in surface reactivity. *J Math Biol* **57,** 333–59 (2008).
12. Wootton, D., Markou, C., Hanso, N. S. & Ku, D. A mechanistic model of acute platelet accumulation in thrombogenic stenoses. *Ann Biomed Eng* **29,** 321–29 (2001).
13. Wang, W., Lindsey, J. P., Chen, J., Diacovo, T. G. & King, M. R. Analysis of early thrombus dynamics in a humanized mouse laser injury model. *Biorheology* **51,** 3–14 (2014).
14. Flamm, M. & Diamond, S. Multiscale systems biology and physics of thrombosis under flow. *Ann Biomed Eng* **40,** 2355–64 (2001).
15. Tahir, H., Bona-Casas, C. & Hoekstra, A. Modelling the effect of a functional endothelium on the development of in-stent restenosis. *PLoS ONE* **8,** e66138 (2013).
16. Wang, W. & King, M. Multiscale modeling of platelet adhesion and thrombus growth. *Ann Biomed Eng* **40,** 2345–2354 (2012).
17. Allender, S. *et al.* European cardiovascular disease statistics 2008. http://hdl.handle.net/10536/DRO/DU:30020501 (2008). European Heart Network, Brussels, England. Date accesed: 12/10/2014.
18. Eckstein, E. On the simultaneous motions of many blood cells. *Bioplhys J* **104,** 1839 (2013).
19. Zhang, G., Zang, S. & B, D. Multiscale particle-based modeling of flowing platelets in blood plasma using dissipative particle dynamics and coarse grained molecular dynamics. *Cell Mol Bioeng* **7,** 552–574 (2014).
20. Zhang, G., Zang, S. & B, D. A multiple time stepping algorithm for efficient multiscale modeling of platelets flowing in blood plasma. *J Comput Phys* **284,** 668–686 (2015).
21. Badimon, L. & Badimon, J. Mechanisms of arterial thrombosis in non parallel streamlines: platelet thrombi grow on the apex of stenotic severely injured vessel wall. experimental study in the pig model. *J CLin Invest* **84,** 1134–44 (1989).
22. Badimon, L., Badimon, J. J., Turitto, V. T. & Fuster, V. Role of von willebrand factor in platelet interaction with an expanded ptfe surface. *ASAIO Trans* **33,** 621–625 (1987).
23. Fernandez-Ortiz, A. *et al.* Characterization of the relative thrombogenicity of atherosclerotic plaque components: Implications for consequences of plaque rupture. *J Am Coll Cardiol* **23,** 1562–1569 (1994).
24. Badimon, J. J., Weng, D., Chesebro, J. H., Fuster, V. & Badimon, L. Platelet deposition induced by severely damaged vessel wall is inhibited by a boroarginine synthetic peptide with antithrombin activity. *Thromb Haemost* **71,** 511–516 (1994).
25. Vilahur, G., Segalés, E., Salas, E. & Badimon, L. Effects of a novel platelet NO-donor (LA816), aspirin, clopidogrel and combined therapy in inhibiting flow and lesion-dependent thrombosis in the porcine *ex vivo* model. *Circulation* **110,** 1686–93 (2004).
26. Pallares, J. & Grau, F. Mass transfer rate of a first-order chemical reaction on a wall at high schmidt numbers. *Int J Heat Mass Transfer* **69,** 438–42 (2014).
27. Tovar-Lopez, F. *et al.* An investigation on platelet transport during thrombus formation at micro-scale stenosis. *PLoS ONE* **8,** e74123 (2013).
28. Colace, T., Tormoen, G., McCarty, O. & Diamond, S. Microfluidics and coagulation biology. *Ann Rev Biomed Eng* **15,** 283–303 (2013).
29. Li, M., Hotaling, N., Ku, D. & Forest, C. Microfluidic thrombosis under multiple shear rates and antiplatelet therapy doses. *PLoS ONE* **9,** e82493 (2014).
30. Badimon, L., Turitto, V., Rosemark, J., Badimon, J. & Fuster, V. Characterization of a tubular flow chamber for studying platelet interaction with biologic and prosthetic materials: Deposition of indium-111 labeled platelets on collagen, subendothelium and expanded polytetrafluoroethylene. *J Lab CLin Med* **110,** 706–18 (1987).
31. Yamaguchi, T. *et al.* Particle-based methods for multiscale modeling of blood flow in the circulation and in devices: challenges and future directions. *Ann Biomed Eng* **38,** 1225–35 (2010).
32. Breiman, L. Random forests. *Machine Learning* **45,** 5–32 (2001).

33. Qi, Y., Bar-Yoseph, P. & Klein-Seetharaman, J. Evaluation of different biological data and computational classification methods for use in protein interaction prediction. *Proteins: Structure, Function and Bioinformatics* **63,** 490–500 (2006).
34. Díaz-Uriarte, R. & Alvarez de Andrés, S. Gene selection and classification of microarray data using Random Forest. *BMC Bioinformatics* **7,** 3 (2006).
35. Strobl, C., Boulesteix, A., Zeileis, A. & Hothorn, T. Bias in random forest variable importance measures: Illustrations, sources and a solution. *BMC Bioinformatics* **8,** 25 (2007).
36. Weiss, H., Turitto, V. & Baumgartner, H. Platelet adhesion and thrombus formation on sub—endothelium in platelets deficient in glycoproteins IIb-IIIa, I b, and storage granules. *Blood* **67,** 322–30 (1986).
37. Markou, C., Hanson, S. & Ku, D. The role of high wall shear rate on thrombus formation in stenoses. *Adv Biomed Eng* **26,** 555–58 (1993).
38. Kilkenny, C., Browne, W. J., Cuthill, I. C., Emerson, M. & Altman, D. G. Improving Bioscience Research Reporting: The ARRIVE Guidelines for Reporting Animal Research. *PLoS Biol* **8,** e00412 (2010).
39. Patel, D. *et al.* Dynamics of GPIIb/IIIa-mediated platelet-platelet interactions in platelet adhesion/thrombus formation on collagen *in vitro* as revealed by videomicroscopy. *Blood* **101,** 929 (2003).
40. David, T., de Groot, P. & Walker, P. Boundary-Layer type solutions for initial platelet activation and deposition. *J Theor Med* **4,** 95–108 (2002).
41. Bark, D. & Ku, D. Platelet transport rates and binding kinetics at high shear over a thrombus. *Biophys J* **105,** 502–11 (2013).
42. Moiseyev, G. & Bar-Yoseph, P. Computational modeling of thrombosis as a tool in the design and optimization of vascular implants. *J Biomech* **46,** 248–52 (2013).
43. Stubley, G., Strong, A., Hale, W. & Absolom, D. A review of mathematical models for the prediction of blood cell adhesion. *Physicochem Hydrodyn* **8,** 221–35 (1987).
44. Zydney, A. & Colton, C. Augmented solute transport in the shear flow of a concentrated suspension. *Physicochem Hydrodyn* **10,** 77–96 (1988).
45. Liaw, A. & Wiener, M. Classification and regression by RandomForest. *R news* **2,** 18–22 (2002).
46. R Core Team. R: A Language and Environment for Statistical Computing. R Foundation for Statistical Computing, Vienna, Austria (2013). http://www.R-project.org/. Date accesed: 07/01/2013.

Acknowledgements

This work was supported by Spanish Ministerio de Economía y Competitividad (MiNECO) grants DPI2010-17212 and CT2013-46799-C2-1-P (to J.P., A.v. and S.C.) and grants FiS2010-18639 and FiS2013-47532-C3 (to R.G. and M.S.-P.), SAF2013-42962-R (to L.B.), SAF-2012-4020\8 (to G.V.), European Union grants PIRG-GA-2010-277166 (to R.G.), PIRG-GA-2010-268342 (to M.S.-P.), and Eu FET grant 817532 (MULTIPLEX) (to R.G., M.S.-P. and A.A.) and a James S. McDonnell Foundation Research Award (to R.G. and M.S.-P.), and generalitat decatalunya Fellowship FI-DGR 2014 (to O.S.). The funders had no role in study design, data collection and analysis, decision to publish, or preparation of the manuscript.

Author Contributions

R.G., M.S.-P. and S.C. designed the research. G.V. and L.B. performed the experiments. J.P., O.S. and S.C. performed the research. A.A.-M. assisted in the research. J.P., O.S., A.V., R.G., A.A.-M., M.S.-P. and S.C. discussed the results. J.P., O.S., R.G., A.V., A.A.-M., G.V., L.B., M.S.-P. and S.C. wrote the paper.

Additional Information

Supplementary information accompanies this paper at http://www.nature.com/srep

Competing financial interests: The authors declare no competing financial interests.

How to cite this article: Pallarès, J. *et al.* A comprehensive study on different modelling approaches to predict platelet deposition rates in a perfusion chamber. *Sci. Rep.* **5**, 13606; doi: 10.1038/srep13606 (2015).